frontiers in Physics

ORIGINAL RESEARCH
published: 24 June 2021
doi: 10.3389/fphy.2021.690721

Generation of High-Order Vortex States From Two-Mode Squeezed States

Graciana Puentes[1,2]* *and Anindya Banerji*[3]

[1]Departamento de Fsica, Facultad de Ciencias Exactas y Naturales, Universidad de Buenos Aires, Ciudad Universitaria, Buenos Aires, Argentina, [2]CONICET-Universidad de Buenos Aires, Instituto de Fsica de Buenos Aires (IFIBA), Ciudad Universitaria, Buenos Aires, Argentina, [3]Centre for Quantum Technologies, National University of Singapore, Singapore, Singapore

We report a scheme for generation of high-order quadrature vortex states using two-mode photon-number squeezed states, generated via the non-linear process of Spontaneous Parametric Down Conversion. By applying a parametric rotation in the quadratures $(\hat{X}, \hat{Y})$, using a ϕ converter, the Gaussian profile of the photon-number squeezed input state can be mapped into a superposition of Laguerre-Gauss modes in the quadratures with N vortices or singularities, for an input state containing $2N$ photons, thus mapping photon-number fluctuations to interference effects in the quadratures. Our scheme has the potential to improve measurement sensitivity beyond the Standard uantum Limit (SQL $\propto \sqrt{N}$), by exploiting the advantages of optical vortices, such as high dimensionality or topological properties, for applications requiring reduced uncertainty, such as quantum cryptography, quantum metrology and sensing.

Keywords: orbital angular momentum, photon-number squeezed states, optical vortices, structured light, spontaneous parametric down conversion

Edited by:
Antonio Zelaquett Khoury, Fluminense Federal University, Brazil

Reviewed by:
Rafael Barros, Tampere University, Finland
Luis Sanchez Soto, Complutense University of Madrid, Spain

***Correspondence:**
Graciana Puentes
gpuentes@df.uba.ar

Specialty section:
This article was submitted to Optics and Photonics, a section of the journal Frontiers in Physics

Received: *04 April 2021*
Accepted: *31 May 2021*
Published: *24 June 2021*

Citation:
Puentes G and Banerji A (2021) Generation of High-Order Vortex States From Two-Mode Squeezed States. Front. Phys. 9:690721. doi: 10.3389/fphy.2021.690721

1 INTRODUCTION

In quantum optics, a beam of light is in a squeezed state if its electric field amplitude has a reduced uncertainty, in relation to that of a coherent state. Thus, the term squeezing refers to squeezed uncertainty. In general, for a classical coherent state with N particles, the sensitivity of a measurement is limited by shot noise to the Standard Quantum Limit (SQL $\propto \sqrt{N}$). On the other hand, quantum states, such as photon-number squeezed states, hold the promise of improving measurement precision beyond the SQL. Squeezed states of light find a myriad of applications, such as in precision measurements, radiometry, calibration of quantum efficiencies, or entanglement-based quantum cryptography, to mention only a few [1–10].

An optical vortex is a singularity or zero point intensity of an optical field. More specific, a generic Laguerre-Gauss beam of order m of the form $\psi \propto e^{im\phi}e^{-r^2}$, with ϕ its azymuthal phase and $r = \sqrt{x^2 + y^2}$ its radial coordinate, has an optical vortex in its center for $m > 0$. The phase in the field circulates around such singularity giving rise to vortices. Integrating around a path enclosing a vortex yields an integer number, multiple of π. This integer is known as the topological charge. There is a broad range of applications of optical vortices in diverse areas, such as in astronomy for detection of extra-solar planets, in optical tweezers for manipulation of cells and micro-particles, in optical communication to improve the spectral efficiency, in Orbital Angular Momentum (OAM) multiplexing, and in quantum cryptography to increase communication bandwidth [11–20].

In this article, we report a scheme for generation of high-order **quadrature** vortex states using two-mode photon-number squeezed states generated *via* the non-linear process of Spontaneous

Parametric Down Conversion (SPDC). By applying a parametric rotation in the quadratures $(\hat{X}, \hat{Y})$ using a ϕ converter, the quadrature representation of the photon-number squeezed input state can be mapped into a vortex state in the quadratures containing N vortices or singularities, for an input state containing $2N$ photons, thus mapping photon-number fluctuations to interference effects in the quadrature, giving rise to the emergence of a state with a well-defined number of vortices. Our scheme has the potential of exploiting the advantages of optical vortices, such as high dimensionality or topological properties, for applications requiring precision beyond the SQL $\propto \sqrt{N}$, such as quantum cryptography, quantum metrology and sensing.

A ϕ converter, also called mode converter, is customarily used in classical optics to convert two orthogonal Hermite-Gauss modes into a Laguerre-Gauss mode. The main motivation of the present work is to explore if an equivalent operation exists that can transform a Hermite-Gauss quadrature representation into a Laguerre-Gauss representation. We found such operation indeed exists. A remarkable feature of this operation is that it can be experimentally realized by using a balanced 50:50 beam splitter. A key application of the scheme reported here is in generation of photon-number squeezed states from quadrature vortex states, by implementation of the inverse protocol.

The article is structured as follows: First, in **Section 2** we review the properties of two-mode photon-number squeezed states such as their quadrature representation and photon-number distribution, second in **Section 3** we introduce the concept of quadrature rotation. Next, in **Section 4**, we present the quadrature representation of the rotated states in terms of Laguerre-Gauss modes. In **Section 5**, we present numerical simulations confirming the creation of N vortices for a squeezed input state containing $2N$ photons. In **Section 6**, we present analytical and numerical derivations for the photon-number distribution of the resulting quadrature vortex states, revealing super-Poissonian photon statistics. Finally, in **Section 7**, we present our conclusions.

2 2-MODE PHOTON-NUMBER SQUEEZED STATE

Consider a truncated two-mode photon-number squeezed state, produced by SPDC, in the Fock state representation of the form [21]:

$$|\psi\rangle = \frac{D}{\cosh r}\sum_{j=0}^{N}(\tanh r)^j |j\rangle_a |j\rangle_b \tag{1}$$

where (a, b) are modes labels, D is a normalization factor and r is the squeezing parameter. In what follows, we consider $|j\rangle_a|j\rangle_b = |j, j\rangle$. The wave-vector and polarization for each mode will be determined by the specific type of SPDC process and configuration being used. For example, in the case of non-collinear type-I SPDC, the two modes would correspond to distinct directions governed by the wave-vectors of signal and idler photons. In order to keep our description as general as possible, we do not limit to a particular SPDC process.

To obtain a quadrature representation of the wavefunction for the state in **Eq. 1**, we use the standard representation of Fock states ($\{|n\rangle\}$) in the position basis ($\{|x\rangle\}$) which, up to a scaling factor, is equivalent to the Hermite-Gauss polynomial of order n, of the form $\langle x|n\rangle = \sqrt{\frac{1}{\pi 2^n n!}}H_n(x)e^{-(x^2)/2}$ [24]. A 2D representation can be obtained by ascribing orthogonal bases ($\{|x, y\rangle\}$) to each mode, where $|x, y\rangle = |x\rangle|y\rangle$ are the eigenvectors of the quadrature operators $\hat{X} = \frac{\hat{a}+\hat{a}^\dagger}{\sqrt{2}}$ and $\hat{Y} = \frac{\hat{b}+\hat{b}^\dagger}{\sqrt{2}}$, with eigenvalues x and y, respectively. Here $(\hat{a}, \hat{b})$ are annihilation operators for the two modes (a, b) [24]. In this notation, the two-mode photon-number states $|n_x, n_y\rangle$ can be written in the quadrature representation as $\langle x, y|n_x, n_y\rangle = \sqrt{\frac{1}{\pi 2^{(n_x+n_y)} n_x! n_y!}}H_{n_x}(x)H_{n_y}(y)e^{-(x^2+y^2)/2}$ [22–25]. Using these expressions, the two-mode photon-number squeezed input state $|\psi\rangle$ has a quadrature representation of the form $\langle x, y|\psi\rangle = \psi(x, y)$:

$$\psi(x, y) = \frac{D}{\cosh r}\sum_{j=0}^{N}(\tanh r)^j \times \sqrt{\frac{1}{\pi 4^j (j!)^2}}H_j(x)H_j(y)e^{-(x^2+y^2)/2}. \tag{2}$$

The quadrature representation of the input state $|\psi\rangle$ is depicted in **Figure 1B** and **Figure 1C**. Such quadrature representation reveals a Gaussian profile, with no vortices or singularities for squeezing parameter $r = 1$. Note that the quadrature profile is not equivalent to the transverse profile of the beam, since $\hat{X}$ and $\hat{Y}$ are quadrature operators, not transvese coordinates. Moreover, the plots in **Figures 1B,C** correspond to the quadrature representation of the wavefunction of the input state $\psi(x, y)$, which is not equivalent to the Wigner function in phase space. The photon-number distribution for the input state $P(n, n) = |\langle n, n|\psi\rangle|^2$ can be calculated obtaining the well known sub-Poissonian quantum statistics. Tracing over one mode we obtain $P(n) = \left|\frac{\tanh r^n}{\cosh r}\right|^2$. Photon-number distributions for different values of the squeezing parameter $r = 1, 0.5, 0.1$ are displayed in **Figure 1D**, revealing thermal statistics when tracing over one mode, while the overall photon-number statistics for the 2-mode squeezed states is sub-Poissonian.

3 QUADRATURE ROTATION

The photon-number squeezed state depicted in **Figure 1** displays a standard Gaussian profile in the quadratures $(\hat{X}, \hat{Y})$, with no topological charges or phase singularities. In order to imprint a vortex in the quadratures $(\hat{X}, \hat{Y})$, we introduce a rotation $\hat{C}$ by an angle ϕ, represented by a unitary operator of the form:

$$\hat{C} = e^{i2\phi\left[\hat{a}^\dagger\hat{b}+\hat{b}^\dagger\hat{a}\right]}, \tag{3}$$

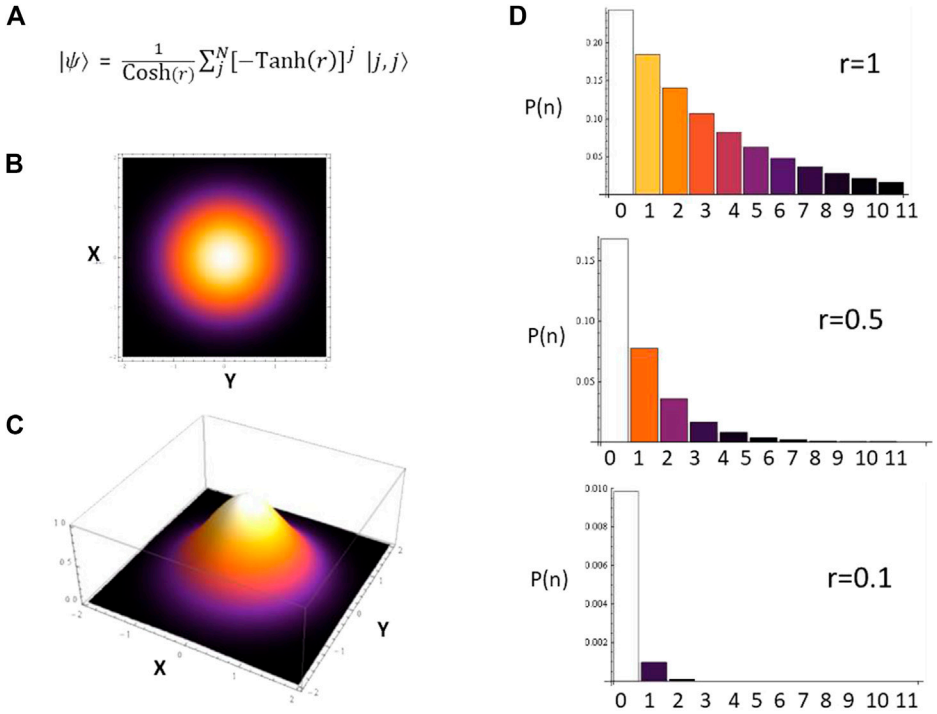

FIGURE 1 | (A) Two-mode photon-number squeezed input state $|\psi\rangle$. **(B,C)** Quadrature representation of input state (not Wigner function) displaying a Gaussian profile with no vortices or singularities, for squeezing parameter $r = 1$. **(D)** Photon-number distribution for different values of squeezing parameter $r = 1, 0.5, 0.1$, revealing thermal statistics by tracing over one mode (see text for details).

where $(\hat{a}^\dagger, \hat{a})$ and $(\hat{b}^\dagger, \hat{b})$ are creation and destruction operators for modes (a, b), which satisfy the standard commutation rules $[\hat{a}^\dagger, \hat{a}] = 1$ and $[\hat{b}^\dagger, \hat{b}] = 1$. Interestingly, $\hat{C}$ is mathematically equivalent to the unitary operator describing the action of a beam splitter in Fock space [1], therefore it can be easily implemented in the laboratory.

The input state transformed under the unitary operator $\hat{C}$ becomes $|\psi'\rangle$:

$$|\psi'\rangle = \hat{C}|\psi\rangle, \tag{4}$$

which represents a rotation of the quadrature by an angle ϕ. In the Heisenberg picture, considering standard commutation rules for creation and annhiliation operators, we obtain the following expression (see **Appendix A**):

$$|\psi'\rangle = \frac{D}{\cosh r}\sum_{j=0}^{N}(\tanh r)^j \times \left(\frac{\hat{a}^\dagger}{\sqrt{2}} + i\,\frac{\hat{b}^\dagger}{\sqrt{2}}\right)^j\left(\frac{\hat{b}^\dagger}{\sqrt{2}} + i\,\frac{\hat{a}^\dagger}{\sqrt{2}}\right)^j|0,0\rangle \tag{5}$$

By a binomial expansion in **Eq. 5** we obtain:

$$|\psi'\rangle = \frac{D}{\cosh r}\sum_{j=0}^{N}A_j^{r,N} \times \sum_{k=0}^{j}\sum_{l=0}^{j}B_{k,l}^{\phi}C_{kl}^{Nj}\big|j-(l-k), j+(l-k)\big\rangle. \tag{6}$$

where D is the normalization factor. The coefficients in the sums are of the form $A_j^{r,N} = (\tanh r)^j\sqrt{\frac{(j)!(j)!}{2^N}}$, $B_{k,l}^{\phi} = (i2\phi)^{l+k}$, while $C_{k,l}^{Nj}$ takes the form (see **Appendix A**):

$$C_{lk}^{Nj} = \frac{\sqrt{(j-l+k)!\,(j+l-k)!}}{k!\,(j-k)!l!\,(j-l)!}. \tag{7}$$

In order to observe the action of the rotation $\hat{C}$ in the quadratures we turn to the quadrature representation of the transformed ket $\langle x, y|\psi'\rangle = \psi'(x, y)$.

4 LAGUERRE-GAUSS MODE EXPANSION

The quadrature representation of the rotated state $\psi'(x, y)$ results in:

$$\psi'(x,y) = \frac{D}{\cosh r}\sum_{j=0}^{N}A_j^{r,N} \times \sum_{k=0}^{j}\sum_{l=0}^{j}B_{k,l}^{\phi}C_{lk}^{Nj}H_{j-(l-k)}(x)H_{j+(l-k)}(y)e^{-\left(x^2+y^2\right)/2}, \tag{8}$$

where $H_{j-(l-k)}(x) = \langle x|j-l+k\rangle$ and $H_{j+(l-k)}(y) = \langle y|j+l-k\rangle$ are Hermite-Gauss polynomials of order $(j-l+k)$ and $(j+l-k)$, respectively.

It is well known that Hermite-Gauss (HG) modes with spatial dependence $H_p(x)H_q(y)$ may become a single Laguerre-Gauss

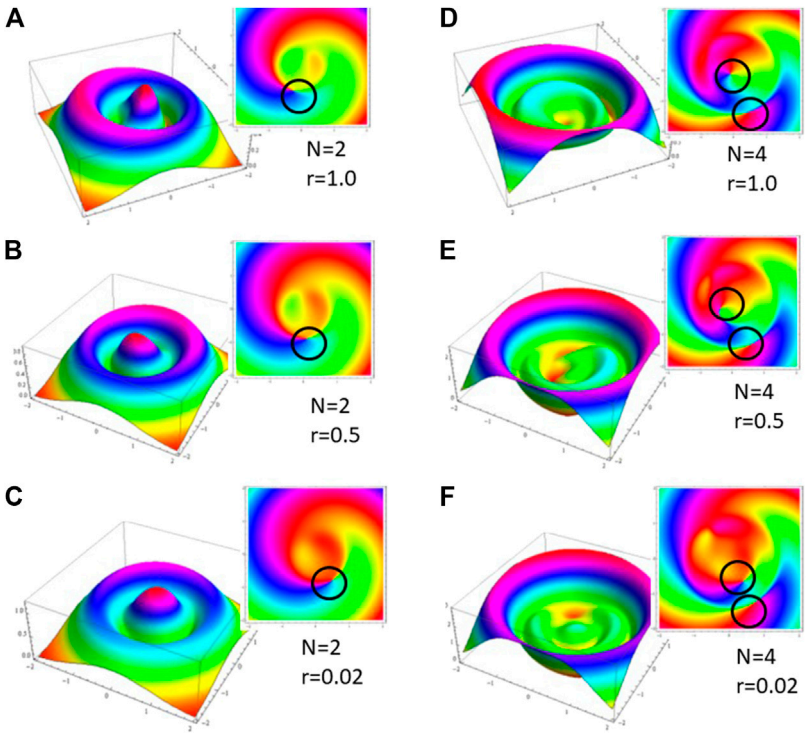

FIGURE 2 | 3D plots of amplitude $|\psi_{LG}(x,y)|$ for resulting Laguerre-Gauss mode in the quadrature representation, depicting the impact of the squeezing parameter r on the formation of vortices, for different values of squeezing parameter r and total photon-number N. Insets correspond to phase profiles $|\phi_{LG}(x,y)|$ for resulting Laguerre-Gauss mode revealing vortices or singularities in the quadratures (not in the transverse profile of the beam). **(A)** $N = 2$, $r = 1$, **(B)** $N = 2$, $r = 0.5$, **(C)** $N = 2$, $r = 0.02$, **(D)** $N = 4$, $r = 1$, **(E)** $N = 4$, $r = 0.5$, **(F)** $N = 4$, $r = 0.02$. As the squeezing parameter decreases, the formation of $N/2$ vortices in the quadratures becomes apparent (see text for details).

(LG) mode of order $L_q^{p-q}(x^2+y^2)$ provided a phase change of $\pi/2$ in the mode profile is achieved [11]. Such Laguerre-Gauss mode is associated with a quadrature vortex number of $(p-q)$ [16, 21–24, 26–34].

By choosing the rotation parameter $\phi = \pi/4$, we may obtain the required phase change to convert the Hermite-Gauss modes into a single Laguerre-Gauss mode. By relabeling the indices $(l-k) = m$, with $m = 0, \ldots, N/2$, we note the quadrature profile can be written as a sum of products of HG modes of the form $H_{j-m}(x)H_{j+m}(y)$. Selecting $\phi = \pi/4$, the quadrature profile can be written in terms of LG modes of the form $L_{j-m}^{2m}(r^2)$, thus resulting in a superposition of LG modes of order $2m$ in the quadrature representation.

5 NUMERICAL RESULTS

To explore the resulting mode-profile in the quadrature $(\widehat{X}, \widehat{Y})$, we performed numerical simulations for a superposition of LG modes of the form:

$$\psi_{LG}(x,y) = \frac{1}{\cosh r}\sum_{j=0}^{N}\sum_{m=0}^{j} A_j^{r,N} C_{kl}^{Nj} \times L_{j-m}^{2m}\left(x^2+y^2\right)e^{-\left(x^2+y^2\right)/2}, \tag{9}$$

where r is the squeezing parameter and the coefficients take the form $A_j^{r,N} = (\tanh r)^j \sqrt{\frac{(j)!\,(j)!}{2^N}}$, $C_{lk}^{Nj} = \frac{\sqrt{(j-l+k)!\,(j+l-k)!}}{k!\,(j-k)!l!\,(j-l)!}$.

We performed numerical simulations in the quadrature for different values of squeezing parameter r, and different values of photon-number N. The results are depicted in **Figure 2** and **Figure 3**. The main result we observe is that, for a sufficiently small squeezing parameter r, the resulting quadrature profile exhibits $N/2$ vortices for an input state with $N/2$ photons *per mode*. In this way, we have mapped the reduced uncertainty in photon-number in Fock space, to a reduced uncertainty in vortex-number in the quadrature.

5.1 Dependence on Squeezing Parameter *r*

In order to better understand the impact of the squeezing parameter r in the formation of vortices in the quadrature, we performed numerical simulations for different squeezing parameters, and for different total number of photons N. This is displayed in **Figures 2A–F**. **Figure 2** left column corresponds to $N = 2$ total photon number and right column corresponds to $N = 4$ total number of photons. Different rows in decreasing order correspond to squeezing parameters $r = 1, 0.5, 0.02$. Numerical simulations clearly reveal that vortices are formed as r decreases, thus as the uncertainty in photon-number decreases, as expected. Thus confirming that the reduced

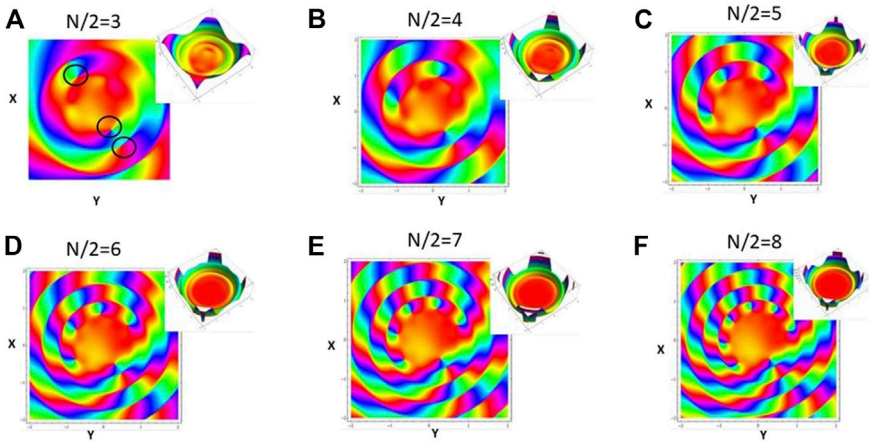

FIGURE 3 | Phase profile $|\phi_{LG}(x,y)|$ of resulting Laguerre-Gauss quadrature representation for a squeezing parameter $r = 0.02$, exploring the impact of the photon-number ($N/2$ per mode) in the formation of vortices. Insets correspond to amplitude plots $|\psi_{LG}(x,y)|$. The numerical results confirm creation of $N/2$ vortices for N total input photons. **(A)** $N/2 = 3$, **(B)** $N/2 = 4$, **(C)** $N/2 = 5$, **(D)** $N/2 = 6$, **(E)** $N/2 = 7$, **(F)** $N/2 = 8$, with $N/2$ input photons per mode (see text for details).

uncertainty in Fock space is mapped to reduced uncertainty in vortex number, in the quadrature.

5.2 Dependence on Photon-Number *N*

To confirm the viability of generation of high-order vortex states in the quadratures we performed numerical simulations for larger total number of photons ($N > 2$). This is depicted in **Figure 3**, for a squeezing parameter $r = 0.02$. **Figures 3A–F** display plots of phase profile associated with $\psi_{LG}(x,y)$, calculated *via* $\phi_{LG}(x,y) = \tan^{-1}\left[\frac{\Im[\psi_{LG}(x,y)]}{\Re[\psi_{LG}(x,y)]}\right]$, for $N/2 = 3,4,5,6,7,8$ input photons per mode, further confirming the azymuthal charge and vorticity in quadrture space increases with the number of photons. Insets display 3D plots of mode amplitude $|\psi_{LG}(x,y)|$. As predicted, in all cases the number of vortices is equal to thel number of photons per mode $N/2$ in the initial 2-mode photon-number squeezed state containing N photons, thus confirming the mapping of photon-number in Fock space to quadrature vortex-number in quadrature.

6 PHOTON-NUMBER DISTRIBUTION OF QUADRATURE VORTEX STATES

The generation of vortices in the quadrature can be considered an interference effect arising from photon-number fluctuations, therefore it is expected that the photon-number distribution should be modified for **quadrature** vortex states. To further confirm that photon-number fluctuations are mapped into interference effects in the quadratures, resulting in the emergence of vortices, for a two-mode photon-number squeezed input state, we calculated the photon-number distribution for the resulting vortex states $P(n_1,n_2) = |\langle n_1,n_2|\psi'\rangle|^2$. Using orthogonality of Fock states, the sums in **Eq. 6** collapse into a single sum, of the form:

$$P(n_1,n_2) = \left|\frac{D}{\cosh r}\sum_{k=0}^{n_1+n_2} A^{N,r}_{n_1,n_2} B^{\phi,k}_{n_1,n_2} C^{N,k}_{n_1,n_2}\right|^2, \tag{10}$$

where $A^{N,r}_{n_1,n_2} = \tanh(r)^{\frac{n_1+n_2}{2}}\sqrt{\frac{(n_1+n_2)!(n_1+n_2)!}{2^N}}$, $B^{\phi,k}_{n_1,n_2} = (i2\phi)^{2k+\frac{n_2-n_1}{2}}$, and $C^{N,k}_{n_1,n_2}$ results in:

$$C^{N,k}_{n_1,n_2} = \frac{\sqrt{(n_1)!(n_2)!}}{\sqrt{k!\left(\frac{n_1+n_2}{2}-k\right)!\left(k+\frac{(n_2-n_1)}{2}\right)!(n_1-k)!}}. \tag{11}$$

Equation 11 reveals the photon-number fluctuations which give rise to the emergence of vortices. Numerical results for the photon-number distributions of quadrature vortex states are presented in **Figure 4** and **Figure 5**, confirming the predicted photon-number fluctuations and super-Poissonian statistics.

In order to further illustrate the photon-number imbalance between the two modes, introduced by the rotation in the quadratures, we performed numerical simulations for the two-mode photon number distribution $P(n_1,n_2)$ for vortex states, taking $n_1 \geq n_2$ and a truncation parameter of N *total* photons in the two-mode state, for a rotation parameter $\phi = \pi/4$. Numerical results for different squeezing parameter values are displayed in **Figure 5**: (a) $N = 6$ and $r = 1.0$, (b) $N = 6$ and $r = 0.5$, (c) $N = 10$ and $r = 1.0$, (d) $N = 10$ and $r = 0.5$. For a sufficiently large squeezing parameter, the photon-number distribution peaks for $n_1 = n_2 \approx N/2$.

7 DISCUSSION

We presented a scheme for generation of high-order quadrature vortex states starting from a two-mode photon-number squeezed state generated *via* the non-linear process of Spontaneous Parametric Down Conversion (SPDC). By applying a parametric rotation in the quadratures $(\hat{X},\hat{Y})$ using a ϕ converter, the quadrature representation of the photon-number squeezed input state is transformed into a high-order **quadrature** vortex state, with N vortices, for an input state containing $2N$ photons, thus mapping the fluctuations in photon-number to interference effects in the quadrature as

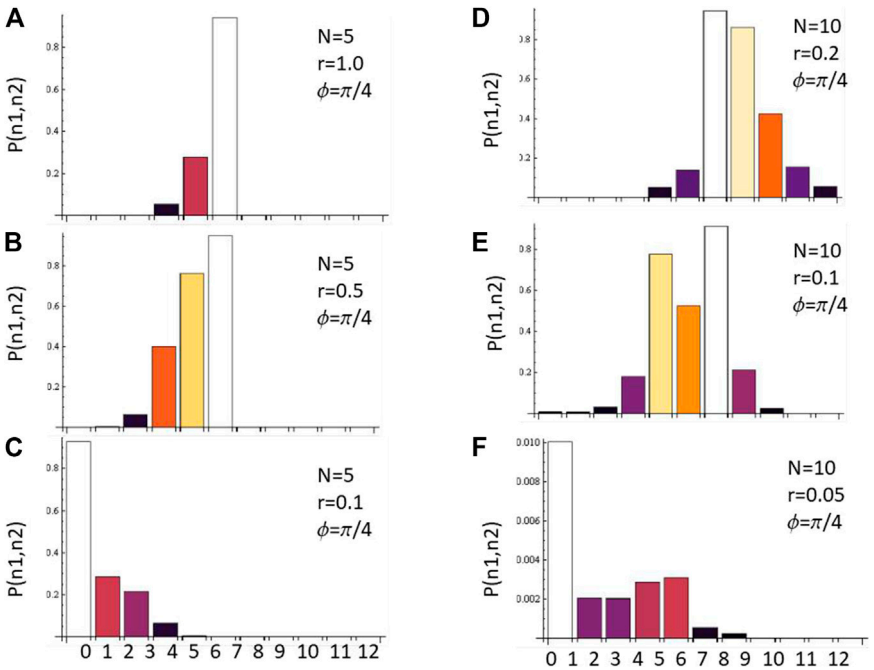

FIGURE 4 | Photon-number statistics $P(n_1, n_2)$ for quadrature vortex states considering $n_1 = n_2$ and a truncation parameter given by N photons *per mode*. Left column $N = 5$ and $\phi = \pi/4$, right column $N = 10$ and $\phi = \pi/4$. Different rows correspond to squeezing parameters **(A)** $r = 1.0$, **(B)** $r = 0.5$, **(C)** $r = 0.1$, **(D)** $r = 0.2$, **(E)** $r = 0.1$, **(F)** $r = 0.05$. The photon-number fluctuations due to quadrature vortex formation is revealed (see text for details).

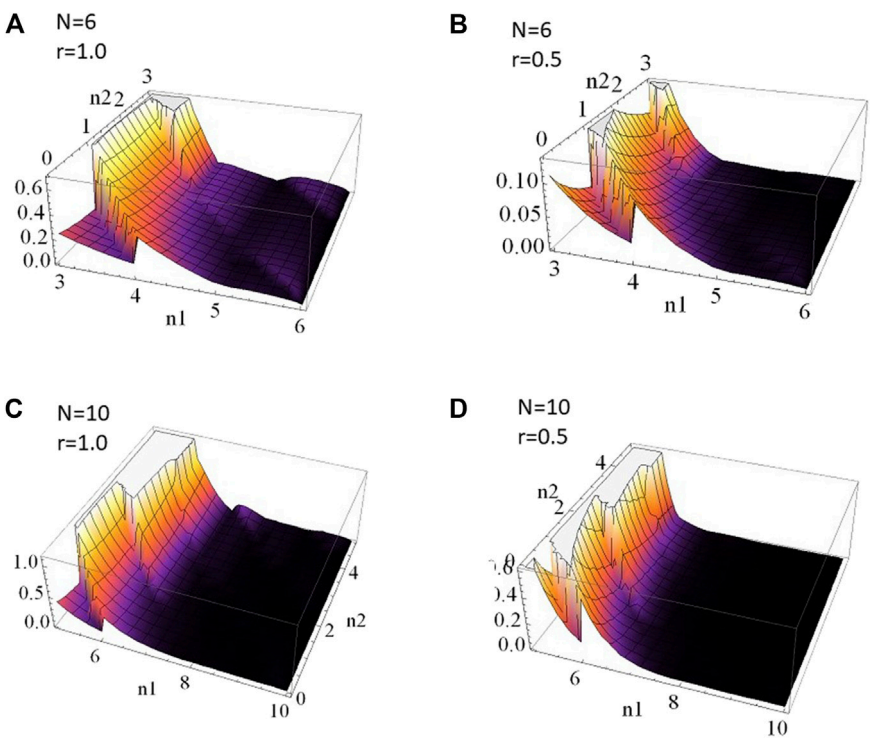

FIGURE 5 | Numerical simulations of photon-number statistics $P(n_1, n_2)$ for quadrature vortex states, taking $n_1 \geq n_2$, and a truncation parameter given by N *total photons* in the two-mode state, for a rotation parameter $\phi = \pi/4$. Numerical results are displayed in Panel 5 for: **(A)** $N = 6$ and $r = 1$, **(B)** $N = 6$ and $r = 0.5$, **(C)** $N = 10$ and $r = 1$, **(D)** $N = 10$ and $r = 0.5$. The photon-number distribution peaks at $n_1 = n_2 \approx N/2$.

depicted by optical singularities with zero-point intensity and singular phase. Furthermore, we obtained analytical and numerical expressions for the super-Poissonian photon-number statistics and fluctuations, giving rise to vortex formation in the quadratures.

Vortex states are customarily generated using various tools, such as Dove prisms, spiral plates, fork holograms, or astigmatic mode converters such as a cylindrical lenses. The important distinction is that these operations act on the transverse profile of the input beam. In the context of the present article, the rotation is performed on the quadrature representation of the state, which can be readily implemented in the lab by a balanced beam splitter. A key application of our scheme is in generation of two-mode photon-number squeezed states from two-mode quadrature vortex states, by implementing the inverse protocol.

Our scheme has the potential of exploiting the advantages of optical vortices, such as high dimensionality and topological properties, for quantum applications requiring squeezed uncertainty beyond the SQL limit ($\sqrt{N}$), such as quantum cryptography, quantum metrology and quantum sensing [35–42].

DATA AVAILABILITY STATEMENT

The data and numerical codes are available upon request.

AUTHOR CONTRIBUTIONS

GP and AB conceived the idea and performed analytical derivations. GP and AB performed numerical simulations. GP wrote the manuscript. All authors provided critical feedback and helped shape the research, analysis and manuscript.

FUNDING

GP acknowledges financial support *via* grants PICT Startup 2015 0710 and UBACyT PDE 2017.

REFERENCES

1. Loudon R. *The Quantum Theory of Light*. 3rd ed. Oxford, United Kingdom: Oxford University Press (2000).
2. Xiao M, Wu L-A, and Kimble HJ. Precision Measurement beyond the Shot-Noise Limit. *Phys Rev Lett* (1987) 59:278–81. doi:10.1103/physrevlett.59.278
3. Walther P, Pan J-W, Aspelmeyer M, Ursin R, Gasparoni S, and Zeilinger A. De Broglie Wavelength of a Non-local Four-Photon State. *Nature* (2004) 429:158–61. doi:10.1038/nature02552
4. McKenzie K, Shaddock DA, McClelland DE, Buchler BC, and Lam PK. Experimental Demonstration of a Squeezing-Enhanced Power-Recycled Michelson Interferometer for Gravitational Wave Detection. *Phys Rev Lett* (2002) 88:231102. doi:10.1103/physrevlett.88.231102
5. Goda K, Miyakawa O, Mikhailov EE, Saraf S, Adhikari R, McKenzie K, et al. A Quantum-Enhanced Prototype Gravitational-Wave Detector. *Nat Phys* (2008) 4:472–6. doi:10.1038/nphys920
6. Ourjoumtsev A, Tualle-Brouri R, Laurat J, and Grangier P. Generating Optical Schrödinger Kittens for Quantum Information Processing. *Science* (2006) 312:83. doi:10.1126/science.1122858
7. Vahlbruch H, Chelkowski S, Hage B, Franzen A, Danzmann K, and Schnabel R. Demonstration of a Squeezed-Light-Enhanced Power- and Signal-Recycled Michelson Interferometer. *Phys Rev Lett* (2005) 95:211102. doi:10.1103/physrevlett.95.211102
8. Wagner K, Janousek J, Delaubert V, Zou H, Harb C, Treps N, et al. Entangling the Spatial Properties of Laser Beams. *Science* (2008) 321:541–3. doi:10.1126/science.1159663
9. Jain N, Huisman SR, Bimbard E, and Lvovsky AI. A Bridge between the Single-Photon and Squeezed-Vacuum States. *Opt Express* (2010) 18:18254–9. doi:10.1364/oe.18.018254
10. Neergaard-Nielsen S, Melholt Nielsen B, Hettich C, Molmer K, and Polzik ES. *Phys Rev Lett* (2006) 97:083604. doi:10.1103/physrevlett.97.083604
11. Allen L, Beijersbergen MW, Spreeuw RJC, and Woerdman JP. Orbital Angular Momentum of Light and the Transformation of Laguerre-Gaussian Laser Modes. *Phys Rev A* (1992) 45:8185–9. doi:10.1103/physreva.45.8185
12. Krenn M, Handsteiner J, Fink M, Fickler R, Ursin R, Malik M, et al. Twisted Light Transmission over 143 Km. *Proc Natl Acad Sci USA* (2016) 113:13648–53. doi:10.1073/pnas.1612023113
13. Paterson L, MacDonald MP, Arlt J, Sibbett W, Bryant PE, and Dholakia K. Controlled Rotation of Optically Trapped Microscopic Particles. *Science* (2001) 292:912. doi:10.1126/science.1058591
14. Wang J, Yang J-Y, Fazal IM, Ahmed N, Yan Y, Huang H, et al. Terabit Free-Space Data Transmission Employing Orbital Angular Momentum Multiplexing. *Nat Photon* (2012) 6:488–96. doi:10.1038/nphoton.2012.138
15. Tian N, Fu L, and Gu M. Resolution and Contrast Enhancement of Subtractive Second Harmonic Generation Microscopy with a Circularly Polarized Vortex Beam. *Sci Rep* (2015) 5:13580. doi:10.1038/srep13580
16. Fickler R, Lapkiewicz R, Plick WN, Krenn M, Schaeff C, Ramelow S, et al. Quantum Entanglement of High Angular Momenta. *Science* (2012) 338:640–3. doi:10.1126/science.1227193
17. Korobchevskaya K, Peres C, Li Z, Antipov A, Sheppard CJR, Diaspro A, et al. Intensity Weighted Subtraction Microscopy Approach for Image Contrast and Resolution Enhancement. *Sci Rep* (2016) 6:25816. doi:10.1038/srep25816
18. Emile O, and Emile J. Naked Eye Picometer Resolution in a Michelson Interferometer Using Conjugated Twisted Beams. *Opt Lett* (2017) 42:354. doi:10.1364/ol.42.000354
19. Fickler R, Campbell G, Buchler B, Lam PK, and Zeilinger A. Quantum Entanglement of Angular Momentum States with Quantum Numbers up to 10,010. *Proc Natl Acad Sci USA* (2016) 113:13642–7. doi:10.1073/pnas.1616889113
20. Padgett MJ. Orbital Angular Momentum 25 Years on [Invited]. *Opt Express* (2017) 25:11265. doi:10.1364/oe.25.011265
21. Caves CM, Zhu C, Milburn GJ, and Schleich W. Photon Statistics of Two-Mode Squeezed States and Interference in Four-Dimensional Phase Space. *Phys Rev A* (1991) 43:3854–61. doi:10.1103/physreva.43.3854
22. Karimi E, Boyd RW, de la Hoz P, de Guise H, Řeháček J, Hradi Z, et al. Radial Quantum Number of Laguerre-Gauss Modes. *Phys Rev A* (2014) 89:8185. doi:10.1103/PhysRevA.89.063813
23. Nienhuis G, and Visser J. Angular Momentum and Vortices in Paraxial Beams. *J Opt A: Pure Appl Opt* (2004) 6:S248–S250. doi:10.1088/1464-4258/6/5/020
24. Agarwal GS, Puri RR, and Singh RP. Vortex States for the Quantized Radiation Field. *Phys Rev A* (1997) 56:4207–15. doi:10.1103/physreva.56.4207
25. Nienhuis G, and Visser J. Angular Momentum and Vortices in Paraxial Beams. *J Opt A: Pure Appl Opt* (2004) 6:S248–S250. doi:10.1088/1464-4258/6/5/020
26. Sanchez-Soto L, Klimov AB, de la Hoz P, Rigas I, Řeháček J, Hradil Z, et al. *Phys Rev A* (2013) 88:053839. doi:10.1103/physreva.88.053839
27. Hemsing E, Knyazik A, Dunning M, Xiang D, Marinelli A, Hast C, et al. Coherent Optical Vortices from Relativistic Electron Beams. *Nat Phys* (2013) 9:549–53. doi:10.1038/nphys2712
28. Mair A, Vaziri A, Weihs G, and Zeilinger A. Entanglement of the Orbital Angular Momentum States of Photons. *Nature* (2001) 412:313–6. doi:10.1038/35085529

29. Oemrawsingh SSR, Aiello A, Eliel ER, Nienhuis G, and Woerdman JP. How to Observe High-Dimensional Two-Photon Entanglement with Only Two Detectors. *Phys Rev Lett* (2004) 92:217901. doi:10.1103/physrevlett.92.217901
30. Marrucci L, Karimi E, Slussarenko S, Piccirillo B, Santamato E, Nagali E, et al. Spin-to-orbital Conversion of the Angular Momentum of Light and its Classical and Quantum Applications. *J Opt* (2011) 13:064001. doi:10.1088/2040-8978/13/6/064001
31. Molina-Terriza G, Rebane L, Torres JP, Torner L, and Carrasco S. *J Eur Opt Soc* (2007) 2:07014. doi:10.2971/jeos.2007.07014
33. Karimi E, and Santamato E. Radial Coherent and Intelligent States of Paraxial Wave Equation. *Opt Lett* (2012) 37:2484. doi:10.1364/ol.37.002484
34. Plick WN, Lapkiewicz R, Ramelow S, and Zeilinger A. The Forgotten Quantum Number: A Short Note on the Radial Modes of Laguerre-Gauss Beams. *arXiv: 1306.6517*.
35. Salomaa MM, and Volovik GE. Quantized Vortices in superfluidHe3. *Rev Mod Phys* (1987) 59:533–613. doi:10.1103/revmodphys.59.533
36. Puentes G, LundeenBranderhorst JSM, Coldesstrodt-Ronge H, Smith B, and Walmsley IA. *Phys Rev Lett* (2009) 102:080404. doi:10.1103/physrevlett.102.080404
37. Puentes G, Datta A, Feito A, Eisert J, Plenio MB, and Walmsley IA. Entanglement Quantification from Incomplete Measurements: Applications Using Photon-Number-Resolving Weak Homodyne Detectors. *New J Phys* (2010) 12:033042. doi:10.1088/1367-2630/12/3/033042
38. Puentes G, Waldherr G, Neumann P, Balasubramanian G, and Wrachtrup J. *Scientific Rep* (2014) 4:1–6. doi:10.1038/srep04677
39. Puentes G, Aiello A, Voigt D, and Woerdman JP. *Phys Rev A* (2007) 75:032319. doi:10.1103/physreva.75.032319
40. Puentes G, Colangelo G, Sewell RJ, and Mitchell MW. Planar Squeezing by Quantum Non-demolition Measurement in Cold Atomic Ensembles. *New J Phys* (2013) 15:103031. doi:10.1088/1367-2630/15/10/103031
41. Moulieras S, Lewenstein M, and Puentes G. Entanglement Engineering and Topological protection by Discrete-Time Quantum Walks. *J Phys B: Mol Opt Phys* (2013) 46:104005. doi:10.1088/0953-4075/46/10/104005
42. Takayama O, and Puentes G. Enhanced Spin Hall Effect of Light by Transmission in a Polymer. *Opt Lett* (2018) 43:1343–6. doi:10.1364/ol.43.001343

Conflict of Interest: The authors declare that the research was conducted in the absence of any commercial or financial relationships that could be construed as a potential conflict of interest.

APPENDIX A

The starting point of the derivation is **Eq. 5**, which defines a $\pi/4$ mode converter:

$$\widehat{C} = \frac{1}{2}\left(\widehat{a}^{\dagger}\widehat{b}^{\dagger} + \widehat{a}^{\dagger}\widehat{b}^{\dagger}\right) \tag{12}$$

where $\widehat{a}^{\dagger}(\widehat{b}^{\dagger})$ are the bosonic mode operators acting on orthogonal modes and follow regular bosonic commutation relations. Also, let us consider the initial state of the two mode system to be the following

$$|\psi\rangle = \sum_j A_j |j\rangle_a |j\rangle_b \tag{13}$$

The above describes a general two-mode state in the Fock basis with total number of particles N distributed between the two modes. Now **Eq. 13** can be written in terms of the mode operators as follows

$$|\psi\rangle = \sum_j A_j (\widehat{a}^{\dagger})^j \left(\widehat{b}^{\dagger}\right)^j |0\rangle_a |0\rangle_b \tag{14}$$

where it is understood that the operator $\widehat{a}^{\dagger}(\widehat{b}^{\dagger})$ acts on mode $|0\rangle_a (|0\rangle_b)$. We want to find how the state $|\psi\rangle$ transforms under the action of $\widehat{C}$. Moving to the Heisenberg picture, the mode operators $\widehat{a}^{\dagger}(\widehat{b}^{\dagger})$ evolve under $\widehat{C}$ as

$$\widehat{a}^{\dagger} \rightarrow \exp\left(i2\phi\widehat{C}\right)\widehat{a}^{\dagger} \exp\left(-i2\phi\widehat{C}^{\dagger}\right) \tag{15}$$

Using the Baker-Hausdorff lemma, we can write **Eq. 15** as follows

$$\exp\left(i2\phi\widehat{C}\right)\widehat{a}^{\dagger} \exp\left(-i2\phi\widehat{C}^{\dagger}\right) = \widehat{a}^{\dagger} + i2\phi\left[\widehat{C}, \widehat{a}^{\dagger}\right] + \tag{16}$$

$$\frac{(i2\phi)^2}{2!}\left[\widehat{C}, \left[\widehat{C}, \widehat{a}^{\dagger}\right]\right] + \ldots \tag{17}$$

Solving for the commutators, we see that $[\widehat{C}, \widehat{a}] = -\widehat{b}^{\dagger}/2$ and. Plugging these values back into **Eq. 16**, we see that we can group the terms as

$$\widehat{a}^{\dagger}\left(1 - \frac{(\phi)^2}{2!} + \ldots\right) - i\widehat{b}^{\dagger}\left(\phi - \frac{\phi^3}{3!} + \ldots\right)$$
$$= \widehat{a}^{\dagger}\cos\phi - i\widehat{b}^{\dagger}\sin\phi \tag{18}$$

Now for a $\pi/4$ mode converter, we put $\phi = \pi/4$ resulting in the transformation

$$\widehat{a}^{\dagger} \rightarrow \frac{1}{\sqrt{2}}\left(\widehat{a}^{\dagger} - i\widehat{b}^{\dagger}\right) \tag{19}$$

and similarly for $\widehat{b}^{\dagger}$. Therefore, **Eq. 14** is transformed to

$$|\psi\rangle_v = \sum_j A_j \left(\widehat{a}^{\dagger} + i\widehat{b}^{\dagger}\right)^j \left(\widehat{b}^{\dagger} + i\widehat{a}^{\dagger}\right)^j |0\rangle_a |0\rangle_b$$

under the effect of the $\pi/4$ mode converter. It is understood in **Eq. 20** that factors $1/\sqrt{2}$ have been absorbed into A_j. **Equation 6** follows from here by a binomial expansion of the terms.